Next, we examined the TNFR1 selectivity of R1-6 based on its structure. Because the structure of TNFR2 is thought to be similar to that of TNFR1,[18] we generated a model structure of TNFR2 by manual mutation based on the crystal structure of TNFR1. This TNF–TNFR2 simulation is speculative, but this model, together with the information obtained from previous mutation studies, can be used to form hypotheses regarding the important structural features for TNFR1 selectivity. The binding surface of TNFR2 was composed of Asp54, Glu57, and Glu70, which could cause a strongly negatively charged surface of TNFR2 different from that of TNFR1 (Fig. 5c and d). Arg31 of wtTNF was thought to have an important role in TNFR2 binding by strongly interacting with this surface (Fig. 5c). R1-6 had an R31A mutation, however, which could cause the loss of the affinity of R1-6 for TNFR2 (Fig. 5d). In support of this finding, a single point mutation R31E mutant was previously reported to have a dramatic loss of affinity for TNFR2.[12,14] On the other hand, the R32W mutant is also reported to be a mutant with TNFR1 selectivity.[12] From our library, Arg32 of our TNFR1-selective candidates was replaced with hydrophobic or nonionic amino acids (Trp, Tyr, Phe, and Gly), which might indicate the importance of Arg32 for binding to TNFR2 (Table 1). This structural information, in combination with bioinformatics technology, will be useful for designing more advanced TNFR-selective mutants and TNFR-selective inhibitors (peptide mimics and chemical compounds).

In conclusion, the phage display technique is an attractive method for creating functional mutants, as demonstrated here by the production of TNFR-specific mutants. Application of this method to various cytokines and proteins will enhance the construction of useful receptor-selective mutants and accelerate functional analysis of these proteins. As an advanced application, analysis of the "structure (sequence)–function relationship" using the obtained mutants will be a powerful technique for basic life science research and drug discovery.

Materials and Methods

Cell culture

HEp-2 cells (a human fibroblast cell line) were provided by the Cell Resource Center for Biomedical Research (Tohoku University) and maintained with RPMI 1640 containing 10% fetal bovine serum and antibiotics. PC60-hTNFR2 cells (a mouse–rat fusion hybridoma comprised of human TNFR2-transfected PC60 cells) were provided by Dr. Vandenabeele and maintained in RPMI 1640 supplemented with 10% fetal bovine serum, 1 mM sodium pyruvate, 5×10^{-5} M 2-mercaptoethanol, 3 μg/ml puromycin, and antibiotics (100 U/ml penicillin, 100 μg/ml streptomycin, and 0.25 μg/ml amphotericin B).

Library construction

The pCANTAB phagemid vector (GE Healthcare Ltd., UK) encoding mutTNF-Lys(−) was used as template for PCR. This TNF was previously reported to be a fully active lysine-deficient TNF mutant.[22] Mutations were introduced in TNF at six amino acid codons (Library I: amino acid residues 29, 31, 32, and 145–147; Library II: amino acid residues 84–89) using a two-step PCR. Three primers, Oligos A, B, and C, were used for the construction of Library I. The first PCR was performed using Oligos A and B. The PCR conditions were 5 min at 95 °C, 35 cycles of denaturization at 95 °C for 15 s, and annealing/extension at 68 °C for 2 min. This first PCR product and Oligo C were then annealed to the template, and PCR was performed again under the same conditions. For the construction of Library II, Oligos A, D, and E were used. The first PCR was performed using Oligos A and D. The first PCR product and Oligo E were used as primers for the second PCR. The PCR conditions of Library II were the same as those of Library I. After the second PCR, the PCR products were digested with HindIII and NotI, and then ligated to a pY03′ phagemid vector (modified from pCANTAB) for the display of TNF variants on the phage surface as g3p fusion proteins. The primer sequences used in this experiment are listed below. Oligos A and E were designed to prime to the pCANTAB vector sequence: Oligo A: 5′-GATAACAA-TTTCACACAGGAAACAGCTATGACCATGATTACGC-CAAGCTTTGGAGCC-3′; Oligo B: 5′-CGCCATTGGCCA-GGAGGGCATTAGCSNNSNNGTTSNNCCACTGGAG-CTGCCCCTCAGCTTGAGGG-3′; Oligo C: 5′-CCAGCG-GATCCGGATACGGCACCGGCGCACCTGCGGCCGC-GGATCCACCACCACCCAGGGCAATGATCCCAAAG-TAGACCTGCCCSNNSNNSNNAAAGTCGAGATA-GTCGGGCCGATTGA-3′; Oligo D: 5′-CTGGCAGGGGC-TGCGGATGGCAGAGAGGAGATTGACGGGSNNSN-NSNNSNNSNNSNNGATGCGGCTGATGGTGTGGG-TGAGGAGCAC-3′; Oligo E: 5′-TGCGGCACGCGGTTC-CAGCGGATC-3′.

Isolation of receptor-selective TNF mutants from the library (affinity panning and screening)

Human TNFR1 Fc (R&D Systems, Inc., Minneapolis, MN) and TNFR2 Fc (R&D Systems, Inc.) were diluted to 50 μg/ml in 10 mM sodium acetate buffer (pH 4.5) and immobilized on a CM3 sensor chip using an amine coupling kit (GE Healthcare Ltd.), which resulted in an increase of 4000–6000 resonance units. The phage library (1×10^{11} colony-forming units/100 μl) was injected at 3 μl/min over the sensor chip. After binding and until the association phase had been reached, the sensor chip was washed using the rinse command and eluted using 20 μl of 10 mM glycine–HCl. The eluted phage was neutralized with 1 M Tris–HCl (pH 6.9). *E. coli* (TG1) was infected with the collected phage for amplification. This panning cycle was performed two more times. After picking up a single clone of transfected *E. coli*, the phagemid vectors were sequenced using a Big Dye Terminator v3.1 kit and ABI PRISM 3100 (Applied Biosystems Ltd., Pleasanton, CA). After the procedure, the binding affinities of the TNF mutants were assessed by ELISA, and their bioactivities through TNFR1 were determined by cytotoxicity assay in human HEp-2 cells.

Expression and purification of TNF mutants

The protocol for the expression and purification of recombinant protein was the same as that described previously.[21,22] Briefly, TNF mutants were produced in the *E. coli* BL21(DE3) strain. The inclusion body of each

TNF mutant was washed in 2.5% Triton X-100 and solubilized in 6 M guanidine–HCl, 0.1 M Tris–HCl (pH 8.0), and 2 mM ethylenediaminetetraacetic acid. Solubilized protein at 10 mg/ml was reduced with 10 mg/ml dithioerythritol for 4 h at room temperature and refolded by 100-fold dilution in a refolding buffer (100 mM Tris–HCl, 2 mM ethylenediaminetetraacetic acid, 0.5 M arginine, and 551 mg/L oxidized glutathione). After dialysis with 20 mM Tris–HCl (pH 7.4) containing 100 mM urea, active trimeric proteins were purified by ion-exchange chromatography using Q-Sepharose FF (GE Healthcare Ltd.). Size-exclusion chromatography was performed using a Superose 12 column (GE Healthcare Ltd.).

In vitro bioactivity of TNF mutants

HEp-2 cells were used for cytotoxicity assay in the presence of cycloheximide (50 μg/ml). HEp-2 cytotoxicity was dependent on TNFR1 signaling. HEp-2 cells were cultured in 96-well plates in the presence of TNF mutants and serially diluted mouse or human wtTNF (PeproTech EC Ltd., UK) at 4×10^4 cells/well. For neutralization assay, cells were cultured in the presence of a constant concentration of human (20 ng/ml) wtTNF and a serial dilution of TNF mutants. After incubation for 18 h, cell survival was determined by methylene blue assay, as described previously.[21,22] To evaluate the bioactivity of the TNF mutant binding specifically to TNFR2, PC60-hTNFR2 cells were used as an index of granulocyte–macrophage colony-stimulating factor (GM-CSF) production, as described previously.[26] Briefly, PC60-hTNFR2 cells were cultured at 5×10^4 cells/well with interleukin-1β (2 ng/ml) and serially diluted TNF mutant. After 24 h of incubation, the amount of rat GM-CSF produced was quantified by ELISA in accordance with the manufacturer's protocol (R&D Systems, Inc.).

Affinity assessment using SPR

The binding kinetics of wtTNF and TNF mutants were analyzed using the BIAcore 3000 SPR system (GE Healthcare Ltd.). TNFRs were immobilized on a CM5 sensor chip, which resulted in an increase of 3000–5000 resonance units. During the association phase, TNF mutants or wtTNF diluted in HBS-EP running buffer (10 mM HEPES pH7.4, 150 mM NaCl, 3 mM EDTA, 0.005% Tween20, GE Healthcare Ltd.) at 78.4, 26.1, or 8.7 nM were individually passed over the immobilized TNFR at a flow rate of 20 μl/min. During the dissociation phase, HBS-EP buffer was applied to the sensor chip at a flow rate of 20 μl/min. The data were analyzed globally with BIAEVALUATION 3.0 software (GE Healthcare Ltd.) using a 1:1 binding model.

Competitive binding of TNF to TNFR1 and TNFR2 (ELISA)

Goat anti-human IgG (MP Biomedicals, Inc., Solon, OH) was immobilized on Maxisorb 96-well ELISA plates (Nalge Nunc International KK, Japan), and nonspecific binding to the plates was blocked using Block Ace (Dainippon Sumitomo Pharma Co., Ltd., Japan). Human TNFR1-Fc or human TNFR2-Fc (ALEXIS Corporation, Switzerland) was bound to coated antibody. Serially diluted TNF with 50 ng/ml FLAG-tagged wtTNF (wtTNF–FLAG) was added to TNFR1-Fc or TNFR2-Fc in 0.4% Block Ace. wtTNF–FLAG binding was detected by anti-FLAG M2 antibody (Sigma-Aldrich Corporation, St. Louis, MO) and avidin horseradish peroxidase conjugate (Invitrogen Corporation, Carlsbad, CA). The binding affinity of TNF was assessed by competitive wtTNF–FLAG binding to TNFR (IC_{50} value).

X-ray crystallography

Purified R1-6 was concentrated to 10 mg/ml in 20 mM Tris–HCl (pH 7.4). Initial screening using a Hampton Crystal screen 1-2 and Crystal screen Lite kit (Hampton Research Corporation, Aliso Viejo, CA) was performed by vapor diffusion method with hanging drops (1+1 μl) at 20 °C. After optimization of the crystallization conditions, rhombohedral crystals (0.2 mm×0.2 mm×0.3 mm) were obtained with reservoir solution containing 0.5 M ammonium sulfate, 1.2 M lithium sulfate, and 0.1 M trisodium citrate (pH 5.6). The crystals were frozen in a cryopreserving solution containing 15% glycerol as cryoprotectant. X-ray diffraction data to 2.5 Å resolution were collected at BL41XU, SPring-8, under flash cooling to 100 K to reduce the effects of radiation damage. Data integration and scaling were performed using HKL2000.[27] Molecular replacement was performed by the MOLREP program in CCP4i[28] using a crystal structure of the wtTNF (1TNF)[25] as search model. Cycles of manual rebuilding using the O program[29] and refinement using the CNS program[30] led to a refined structure. Final refinement (TLS refinement) was performed using the Refmac program in CCP4i.[28] Final model validation was performed using PROCHECK program in CCP4i.[28] The model complexes of TNF–TNFR1 and R1-6–TNFR1 were constructed based on the crystal structure of the LTα–TNFR1 complex[18] using the superimposing program in CCP4i. Structural models of TNFR2 were constructed based on the TNFR1 structure by manual mutation using the O program.[29]

Accession number

Coordinates and structure factors have been deposited in the PDB with accession number 2ZJC.

Acknowledgements

This study was supported by Research for Promoting Technological Seeds (no. 11-067) from the Japan Science and Technology Agency; Research Fund Project on Health Sciences focusing on Drug Innovation (no. KAA3701) from the Japan Health Sciences Foundation; the Global COE Program "*In Silico* Medicine" (Wakate-16) at Osaka University; a Grant-in-Aid for Young Scientists (B) (no. 20790134) and Grants-in-Aid for Scientific Research (nos. 18015055 and 17689008) from the Ministry of Education, Culture, Sports, Science, and Technology of Japan; and Research Fellowships for Young Scientists (no. 20-3919) from the Japan Society for the Promotion of Science.

References

1. Aggarwal, B. B. (2003). Signalling pathways of the TNF superfamily: a double-edged sword. *Nat. Rev. Immunol.* **3**, 745–756.

2. Feldmann, M. & Maini, R. N. (2003). Lasker Clinical Medical Research Award. TNF defined as a therapeutic target for rheumatoid arthritis and other autoimmune diseases. *Nat. Med.* **9**, 1245–1250.
3. Kooloos, W. M., de Jong, D. J., Huizinga, T. W. & Guchelaar, H. J. (2007). Potential role of pharmacogenetics in anti-TNF treatment of rheumatoid arthritis and Crohn's disease. *Drug Discov. Today*, **12**, 125–131.
4. Rutgeerts, P., Van Assche, G. & Vermeire, S. (2004). Optimizing anti-TNF treatment in inflammatory bowel disease. *Gastroenterology*, **126**, 1593–1610.
5. Rothe, J., Lesslauer, W., Lötscher, H., Lang, Y., Koebel, P., Köntgen, F. *et al.* (1993). Mice lacking the tumour necrosis factor receptor 1 are resistant to TNF-mediated toxicity but highly susceptible to infection by *Listeria monocytogenes*. *Nature*, **364**, 798–802.
6. Kafrouni, M. I., Brown, G. R. & Thiele, D. L. (2003). The role of TNF–TNFR2 interactions in generation of CTL responses and clearance of hepatic adenovirus infection. *J. Leukocyte Biol.* **74**, 564–571.
7. Rahman, M. M. & McFadden, G. (2006). Modulation of tumor necrosis factor by microbial pathogens. *PLoS Pathog.* **2**, e4.
8. Chan, F. K., Shisler, J., Bixby, J. G., Felices, M., Zheng, L., Appel, M. *et al.* (2003). A role for tumor necrosis factor receptor-2 and receptor-interacting protein in programmed necrosis and antiviral responses. *J. Biol. Chem.* **278**, 51613–51621.
9. Wajant, H., Pfizenmaier, K. & Scheurich, P. (2003). Tumor necrosis factor signaling. *Cell Death Differ.* **10**, 45–65.
10. Weiss, T., Grell, M., Siemienski, K., Mühlenbeck, F., Dürkop, H., Pfizenmaier, K. *et al.* (1998). TNFR80-dependent enhancement of TNFR60-induced cell death is mediated by TNFR-associated factor 2 and is specific for TNFR60. *J. Immunol.* **161**, 3136–3142.
11. Fotin-Mleczek, M., Henkler, F., Samel, D., Reichwein, M., Hausser, A., Parmryd, I. *et al.* (2002). Apoptotic crosstalk of TNF receptors: TNF-R2-induces depletion of TRAF2 and IAP proteins and accelerates TNF-R1-dependent activation of caspase-8. *J. Cell Sci.* **115**, 2757–2770.
12. Van Ostade, X., Vandenabeele, P., Everaerdt, B., Loetscher, H., Gentz, R., Brockhaus, M. *et al.* (1993). Human TNF mutants with selective activity on the p55 receptor. *Nature*, **361**, 266–269.
13. Barbara, J. A., Smith, W. B., Gamble, J. R., Van Ostade, X., Vandenabeele, P., Tavernier, J. *et al.* (1994). Dissociation of TNF-alpha cytotoxic and pro-inflammatory activities by p55 receptor- and p75 receptor-selective TNF-alpha mutants. *EMBO J.* **13**, 843–850.
14. Van Ostade, X., Vandenabeele, P., Tavernier, J. & Fiers, W. (1994). Human tumor necrosis factor mutants with preferential binding to and activity on either the R55 or R75 receptor. *Eur. J. Biochem.* **220**, 771–779.
15. Van Ostade, X., Tavernier, J. & Fiers, W. (1994). Structure–activity studies of human tumour necrosis factors. *Protein Eng.* **7**, 5–22.
16. Yamagishi, J., Kawashima, H., Matsuo, N., Ohue, M., Yamayoshi, M., Fukui, T. *et al.* (1990). Mutational analysis of structure–activity relationships in human tumor necrosis factor-alpha. *Protein Eng.* **3**, 713–719.
17. Zhang, X. M., Weber, I. & Chen, M. J. (1992). Site-directed mutational analysis of human tumor necrosis factor-alpha receptor binding site and structure–functional relationship. *J. Biol. Chem.* **267**, 24069–24075.
18. Banner, D. W., D'Arcy, A., Janes, W., Gentz, R., Schoenfeld, H. J., Broger, C. *et al.* (1993). Crystal structure of the soluble human 55 kD TNF receptor-human TNF beta complex: implications for TNF receptor activation. *Cell*, **73**, 431–445.
19. Fu, Z. Q., Harrison, R. W., Reed, C., Wu, J., Xue, Y. N., Chen, M. J. & Weber, I. T. (1995). Model complexes of tumor necrosis factor-alpha with receptors R1 and R2. *Protein Eng.* **8**, 1233–1241.
20. Reed, C., Fu, Z. Q., Wu, J., Xue, Y. N., Harrison, R. W., Chen, M. J. & Weber, I. T. (1997). Crystal structure of TNF-alpha mutant R31D with greater affinity for receptor R1 compared with R2. *Protein Eng.* **10**, 1101–1107.
21. Shibata, H., Yoshioka, Y., Ikemizu, S., Kobayashi, K., Yamamoto, Y., Mukai, Y. *et al.* (2004). Functionalization of tumor necrosis factor-alpha using phage display technique and PEGylation improves its anti-tumor therapeutic window. *Clin. Cancer Res.* **10**, 8293–8300.
22. Yamamoto, Y., Tsutsumi, Y., Yoshioka, Y., Nishibata, T., Kobayashi, K., Okamoto, T. *et al.* (2003). Site-specific PEGylation of a lysine-deficient TNF-alpha with full bioactivity. *Nat. Biotechnol.* **21**, 546–552.
23. Shibata, H., Yoshioka, Y., Ohkawa, A., Minowa, K., Mukai, Y., Abe, Y. *et al.* (2008). Creation and X-ray structure analysis of the tumor necrosis factor receptor-1-selective mutant of a tumor necrosis factor-alpha antagonist. *J. Biol. Chem.* **283**, 998–1007.
24. Loetscher, H., Stueber, D., Banner, D., Mackay, F. & Lesslauer, W. (1993). Human tumor necrosis factor alpha (TNF alpha) mutants with exclusive specificity for the 55-kDa or 75-kDa TNF receptors. *J. Biol. Chem.* **268**, 26350–26357.
25. Eck, M. J. & Sprang, S. R. (1989). The structure of tumor necrosis factor-alpha at 2.6 A resolution. Implications for receptor binding. *J. Biol. Chem.* **264**, 17595–17605.
26. Abe, Y., Yoshikawa, T., Kamada, H., Shibata, H., Nomura, T., Minowa, K. *et al.* (2008). Simple and highly sensitive assay system for TNFR2-mediated soluble- and transmembrane-TNF activity. *J. Immunol. Methods*, **335**, 71–78.
27. Otwinowski, Z. & Minor, W. (1997). Processing of X-ray diffraction data collected in oscillation mode. *Methods Enzymol.* **276**, 307–326.
28. Potterton, E., Briggs, P., Turkenburg, M. & Dodson, E. (2003). A graphical user interface to the CCP4 program suite. *Acta Crystallogr. Sect. D*, **59**, 1131–1137.
29. Jones, T. A., Zou, J. Y., Cowan, S. W. & Kjeldgaard, M. (1991). Improved methods for building protein models in electron density maps and the location of errors in these models. *Acta Crystallogr. Sect. A*, **47** (Pt 2), 110–119.
30. Brunger, A. T., Adams, P. D., Clore, G. M., DeLano, W. L., Gros, P., Grosse-Kunstleve, R. W. *et al.* (1998). Crystallography and NMR system: a new software suite for macromolecular structure determination. *Acta Crystallogr. Sect. D*, **54**, 905–921.

TECHNICAL BRIEF

Improved protein sequence coverage by on resin deglycosylation and cysteine modification for biomarker discovery

Haruhiko Kamada[1, 2], *Tim Fugmann*[1], *Dario Neri*[1] *and Christoph Roesli*[1]

[1] Department of Chemistry and Applied Biosciences, ETH Zurich, Zurich, Switzerland
[2] Laboratory of Pharmaceutical Proteomics, National Institute of Biomedical Innovation, Osaka, Japan

Received: May 29, 2008
Revised: August 18, 2008
Accepted: September 15, 2008

Membrane proteins and secreted factors (soluble proteins or extracellular matrix components) are the targets of most monoclonal antibodies, which are currently in clinical development. These proteins are frequently post-translationally modified, *e.g.* by the formation of disulfide bonds or by glycosylation, which complicates their identification using proteomics technologies. Here, we describe a novel methodology for the on resin deglycosylation and cysteine modification of proteins after *in vitro*, *in vivo* or *ex vivo* biotinylation. Biotinylated proteins are captured on streptavidin resin and all subsequent modifications, as well as the proteolytic digestion, which yields peptides for MS analysis, are performed on resin. Using biotinylated bovine fetuin-A as a test protein, an improvement in sequence coverage from 7.9 to 58.7% could be shown, including the identification of all three glycosylation sites. Furthermore, a complex mixture derived from the *ex vivo* biotinylation of vascular structures in human kidney with cancer obtained by perfusion after surgical resection revealed almost a doubling of sequence coverage for all checked proteins when analyzed by LC-MALDI TOF/TOF.

Keywords:
Biotinylation / Cysteine modification / Deglycosylation / MALDI-TOF/TOF / On resin

The identification of disease-associated membrane proteins and secreted factors represents an area of intense pharmaceutical research activity, because these targets can often be drugged using human mAb [1, 2]. In particular, there is a growing interest in the characterization of proteins, which are accessible in the vascular bed and in the peri-vascular extracellular matrix (ECM), because of the recognition that vascular alterations are often associated to pathological conditions and in consideration of the ready accessibility of these structures *in vivo* [3]. Proteomics studies with membrane proteins, secreted proteins and ECM components are often hindered by problems of low abundance, limited solubility in water and/or PTM, including the attachment of oligosaccharides (glycosylation) to specific amino acids in proteins. Indeed, both disulfide bond formation and glycosylation significantly influence protein folding, stability and activity [4], but at the same time may complicate proteomics studies by hindering proteolytic digestion, peptide recovery and analysis. While proteins can exhibit both *O*-linked and *N*-linked glycosylation, we focused on the *N*-glycosidic linkage, which is found on asparagines in the consensus sequence N-X-S(T), where X is any amino acid except proline [5], because of its prominence in mammalian proteins. The removal of *N*-linked glycan chains is usually performed by PNGase F treatment, an amidase that cleaves between the

Correspondence: Dr. Christoph Roesli, Institute of Pharmaceutical Sciences, Swiss Federal Institute of Technology Zurich, Wolfgang-Pauli-Str. 10, HCI G392.4, 8093 Zurich, Switzerland
E-mail: christoph.roesli@pharma.ethz.ch
Fax: +41-44-633-1358

Abbreviations: **ECM**, extracellular matrix; **NEM**, N-ethylmaleimide; **TCEP**, tris-(2-carboxyethly)phosphine

innermost GlcNAc and asparagine residues [6]. As a result of this cleavage, the originally glycosylated asparagine residue is hydrolyzed to an aspartic acid, which can easily be detected by MS/MS.

Similarly, the MS identification of proteins containing disulfide bonds is hampered by a reduced digestion efficacy and the cross-linking of peptides [7]. Therefore, many proteomics projects rely on the reduction of these S-S bonds followed by the covalent modification of reduced cysteines preventing the rearrangement of disulfide bridges. From the variety of possible reducing agents and modification reagents, we chose Tris-(2-carboxyethly)phosphine (TCEP) as reducing agent and N-ethylmaleimide (NEM) for the thiol-selective modification (formation of a thiolether).

During the last years, our lab has developed proteomics technologies for the covalent biotinylation (*in vitro* [8, 9], *in vivo* [10-12] and *ex vivo* [13]) of accessible proteins and their subsequent enrichment, as well as for the relative quantification of these proteins [9, 14]. To obtain increased numbers of identified proteins and improved sequence coverage, we now integrated an on resin cysteine modification step followed by the treatment of proteins with PNGase F for the removal of *N*-linked glycans into our established protocol.

Figure 1 shows a scheme of the newly developed enrichment and modification procedure. Briefly, proteins were covalently modified with a reactive ester derivative of biotin and captured on streptavidin resin. Following a stringent wash protocol, disulfide bonds were reduced with TCEP and modified with NEM. After PNGase F treatment for the digestion of *N*-linked glycans, an on resin proteolysis step was performed. The resulting tryptic peptides were then analyzed by MALDI-TOF MS.

We first implemented the cysteine modification and PNGase F treatment method on bovine protein α-2-HS-glycoprotein (fetuin-A, obtained from Sigma-Aldrich), a protein with three *N*-linked and three *O*-linked glycans [15] and with 12 cysteine residues involved in the formation of six intramolecular disulfide bonds [16]. The glycoprotein was dissolved in PBS and primary amines (lysine side-chains and the N terminus) were covalently modified with sulfosuccinimidyl-6-(biotinamide)-hexanoate (sulfo-NHS-LC-biotin, Thermo Fisher Scientific). On average, two biotin molecules were attached to each molecule of fetuin-A (confirmed by linear MS analysis). Biotinylated fetuin-A was then captured on streptavidin Sepharose (GE Healthcare) and the resin was stringently washed according to published procedures [10]. To reduce the disulfide bonds, the Sepharose was incubated in PBS containing 5 mM TCEP for 10 min at 70°C. TCEP was preferred to other sulfur-containing reducing agents, since it is widely used in cysteine reducing procedures and since it does not contain thiol moieties, which could react with alkylating agents. Following incubation with 0.25 μmol NEM (Thermo Fisher Scientific) for 2 h at room temperature (RT) the reaction was stopped by the addition of 0.25 μmol cysteine. In our hands, NEM worked better compared to other alkylating reagents tested (NEM, IAA and MMTS).

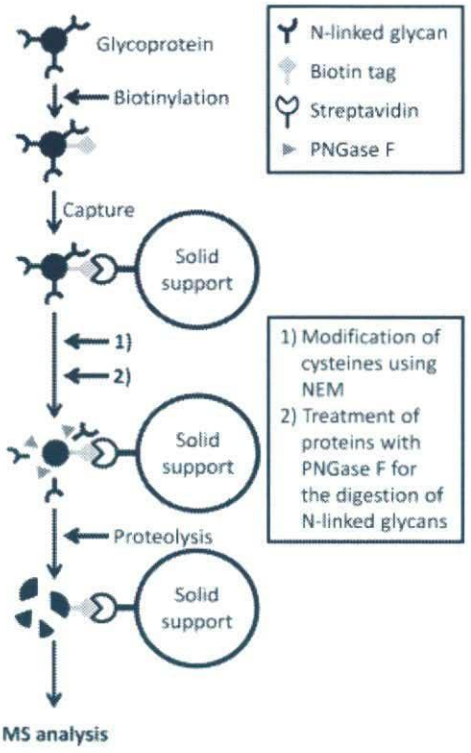

Figure 1. Schematic representation of the experimental methodology. Proteins are either biotinylated in solution, *in vitro*, *in vivo* or *ex vivo* before being captured on streptavidin Sepharose resin. All subsequent modification steps are performed on resin allowing the use of optimal buffer systems. After reduction of disulfide bonds, the cysteines are modified using NEM. Following treatment of the proteins with PNGase F for the digestion of *N*-linked glycans, an on resin proteolytic digestion using the endopeptidase trypsin is carried out. Resulting peptides can easily be separated from the resin and analyzed by MS.

After washing the resin three times with PNGase F digestion buffer (1% NP-40, 0.5% SDS w/v, 40 mM DTT in PBS), the deglycosylation was carried out for 1 h at RT using 1 μL of PNGase F stock solution (500 000 units/mL, New England BioLabs). The resin was then washed three times with trypsin digestion buffer (50 mM Tris-HCl pH 8.0, 1 mM $CaCl_2$ in MilliQ water) and the digestion was performed overnight with 200 ng of sequencing grade modified trypsin (trypsin : fetuin-A ratio = 1 : 320; Promega) in an orbital shaker (1000 rpm) at 37°C (Eppendorf). Supporting Information Fig. 1 shows that sequence coverage is essentially stable in a broad range of trypsin:protein ratios, taking the number of identified fetuin-A peptides as an example. The resulting tryptic peptides were desalted and concentrated using ZipTips (Eppendorf) according to the manufacturer's instructions. The lyophilized peptides were dissolved in matrix buffer (70% ACN, 0.1% TFA in MilliQ water), mixed with 3 mg/mL CHCA and spotted onto a 384-well MALDI target plate (Applied Biosystems). MALDI-TOF/TOF analysis was carried out with the 4800 MALDI TOF/TOF Analyzer (Applied Bio-

systems). All spectra were acquired with a solid-state laser (355 nm) at a laser repetition rate of 200 Hz. After measuring all samples in the MS mode, a maximum of 15 precursors per spot were selected for subsequent fragmentation by CID. The resulting spectra were processed and analyzed using the Global Protein Server Workstation (Applied Biosystems), which uses internal MASCOT (Matrix Sciences) software for matching MS and MS/MS data against databases of *in silico* digested proteins. The data obtained were screened against a database of all known proteins downloaded from the Expasy homepage (http://www.expasy.org). The search was restricted to mammalian proteins. Furthermore, following analysis settings were used for the identification of peptides and proteins: (i) precursor tolerance: 30 ppm, (ii) MS/MS fragment tolerance: 0.2 Da, (iii) maximal missed cleavages: 2 and (iv) three variable modifications [NEM, PNGase F (conversion of Asn to Asp) and oxidation of methionine]. Peptides were considered correct calls when the confidence interval was greater than 95%.

Figure 2A shows two representative MS-spectra of fetuin-A processed according to the standard protocol (no cysteine modification and no PNGase F treatment, left spectrum) and the optimized protocol (cysteine modification with TCEP and NEM as well as PNGase F treatment, right spectrum). Identified peptides are marked with empty and closed circles for the standard protocol and the optimized protocol, respectively. Figure 2B indicates the peptides of fetuin-A identified using the standard protocol (filled squares) or the new optimized protocol (empty squares). After cleavage of the signal sequence, fetuin-A comprises 341 amino acid residues. Using the standard protocol, only 27 of them (without any cysteine and any *N*-linked glycosylation site) could be annotated (sequence coverage: 7.9%). Using on resin cysteine modification and deglycosylation with PNGase F, 200 residues (sequence coverage: 58.7%), eight out of twelve cysteines and all sites of *N*-linked glycosylation were identified. The quality of the MS/MS spectra is documented in Supporting Information Fig. 2, which shows the assignment of the PTM at position 17 of the peptide VVHAVEVALATFNAESN*GSYLQLVEISR of fetuin-A.

Encouraged by these results, we transferred the optimized protocol to the analysis of complex samples. As previously published [13], we analyzed human surgically resected tumor bearing kidneys, which were perfused *ex vivo* with the commercial active ester derivative of biotin sulfo-NHS-LC-biotin (Thermo Fisher Scientific). Four different proce-

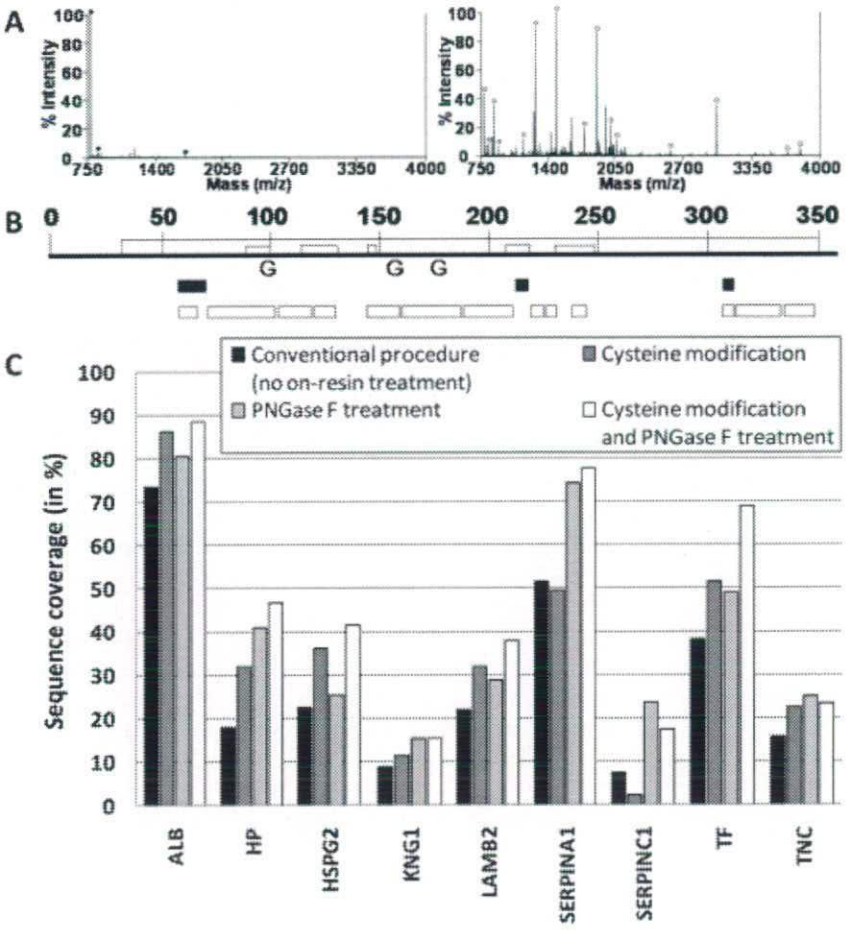

Figure 2. Analysis of sequence coverage changes. (A) Two representative MALDI spectra obtained from bovine fetuin-A. The left spectrum was obtained after on resin proteolytic digestion of biotinylated fetuin-A without any further modification (conventional procedure). Identified peptides are marked with black circles. The right spectrum shows fetuin-A peptides (marked with open circles) after on resin cysteine modification, PNGase F treatment and tryptic digestion (optimized procedure). (B) Graphic representation of fetuin-A. Disulfide bonds are indicated with vertical bars and *N*-linked glycosylation sites are marked with "G". All peptides annotated to fetuin-A in panel A are indicated (conventional procedure: black squares, optimized procedure: white squares). (C) Histogram of sequence coverages for selected, representative proteins identified from a complex sample (*ex vivo* biotinylated surgical resected human tumor-bearing kidneys).

dures were tested: (i) a conventional protocol [10] without cysteine modification and deglycosylation, (ii) on resin cysteine modification only, (iii) on resin PNGase F treatment only and (iv) the combination of on resin cysteine modification and PNGase F treatment (optimized protocol). For each sample, 5 mg of total protein extracts was subjected to capture on streptavidin Sepharose. After stringent washing steps with three different buffers [1% NP-40, 0.1% SDS in PBS, followed by 0.1% SDS, 2 M NaCl in PBS (40°C) and for (i): 50 mM Tris-HCl, 1 mM $CaCl_2$ in MilliQ water (pH 8.0); for (ii) and (iv): 100 mM phosphate buffer containing 5 mM TCEP; for (iii): 0.5% SDS, 40 mM DTT in PBS], the four different treatment procedures were performed as described above. After overnight proteolytic digestion, tryptic peptides were concentrated using C18 OMIX 100 μL tips (Varian) according to the manufacturer's instructions. The lyophilized peptides were dissolved in 12 μL mobile phase A buffer (5% ACN, 0.1% TFA in MilliQ water) and separated by RP HPLC using an UltiMate nanoscale LC system and a FAMOS microautosampler (Dionex) controlled by the Chromeleon software (Dionex). Mobile phase B consisted of 80% ACN and 0.1% TFA in MilliQ water. The flow rate was set to 300 nL/min. Five microliter of each sample was loaded on the column (15 cm × 75 μm id, C18 PepMap 100, 3 μm, and 100 Å; Dionex). Peptides were eluted with a gradient of 0% buffer B for 3 min, 0–52% buffer B for 187 min, 52–100% buffer B for 10 min, and 100% buffer B for 5 min; the column was equilibrated with 100% buffer A for 34 min before the next sample was analyzed. The eluted fractions were mixed with a solution of 3 mg/mL CHCA, 277 pmol/mL of each of the four peptides used as internal standard ([8], [des-arg^9]-bradykinin, neurotensin, angiotensin I, and adrenocorticotropic hormone fragment 1-17; all from Sigma)], 70% ACN, and 0.1% TFA in MilliQ water and were deposited on a 1664-well MALDI target plate using the online Probot robotic spotting system (Dionex). The flow of the MALDI matrix solution was set to 1083 nL/min and therefore, each fraction collected for 10 s contained 180.5 nL MALDI-matrix and 50 nL sample. The final concentration of each of the three standard peptides was 50 fmol per spot. The MALDI-TOF and MALDI-TOF/TOF MS analyses were carried out as described above. The MASCOT search parameters for these samples were (i) a human database downloaded from the European Bioinformatics Institute homepage (ftp://ftp.ebi.ac.uk/pub/databases/SPproteomes/fasta/ proteomes/25.H_sapiens.fasta.gz); (ii) allowed number of missed cleavages: one; (iii) variable PTM: NEM, PNGase F (conversion of Asn to Asp) and oxidation of methionine; (iv) peptide tolerance: ±10 ppm; (v) MS/MS tolerance: ±0.25 Da; and (vi) peptide charge: +1. Peptides were selected for analysis if identified with a confidence interval of >95%, using the MOWSE scoring algorithm, which calculates protein identification probability [17]. The reduction of redundancy as well as the comparison of the different samples was performed using the ProteinCenter software (Proxeon).

Figure 2C shows the changes in sequence coverage for a number of selected, representative proteins. On average, the sequence coverage was improved by 80% for the optimized protocol (cysteine modification in combination with PNGase F treatment) compared to the standard protocol (no on-resin treatment). Supporting Information Fig. 3 presents the identified peptides for selected regions of the proteins indicated in Fig. 2C. A substantial increase in both numbers of identified glycosylation sites as well as the number of cysteine residues taking part in disulfide bond formation could be observed. For illustration how MALDI-TOF/TOF data can be used to assign glycosylation sites, representative MS/MS spectra of selected *N*-glycosylated peptides are shown in Supporting Information Fig. 4.

We have successfully used this new procedure for the on resin deglycosylation and cysteine modification both using purified proteins and complex protein mixtures from *ex vivo* biotinylation procedures. We are presently applying the optimized protocol to a number of large-scale comparative analyses of human, mouse and rat tissues. As protein biotinylation procedures are frequently performed in order to enrich an accessible subset of the proteome for biomarker discovery and for basic biology studies, we anticipate that the on resin procedure described in this Technical Brief may find a broad applicability in many proteomics laboratories.

Financial support from ETH, the Swiss National Science Foundation, the Gebert-Rüf Foundation, the Bundesamt für Bildung und Wissenschaft (EU Project STROMA), the European Union (EU Projects Immuno-PDT and DiaNa) is gratefully acknowledged. This work was supported in part by a Health and Labour Sciences Research Grants in Japan and a Japan Food Hygiene Association Grant for Promoted Project of Research on Risk of Chemical Substances. We thank the Functional Genomics Center Zurich for access to instrumentation and technical support.

The authors have declared no conflict of interest.

References

[1] Carter, P. J., Potent antibody therapeutics by design. *Nat. Rev.* 2006, *6*, 343–357.

[2] Schrama, D., Reisfeld, R. A., Becker, J. C., Antibody targeted drugs as cancer therapeutics. *Nat. Rev. Drug Discov.* 2006, *5*, 147–159.

[3] Neri, D., Bicknell, R., Tumour vascular targeting. *Nat. Rev. Cancer* 2005, *5*, 436–446.

[4] Matsumura, M., Signor, G., Matthews, B. W., Substantial increase of protein stability by multiple disulphide bonds. *Nature* 1989, *342*, 291–293.

[5] Jenkins, N., Parekh, R. B., James, D. C., Getting the glycosylation right: implications for the biotechnology industry. *Nat. Biotechnol.* 1996, *14*, 975–981.

[6] Tarentino, A. L., Gomez, C. M., Plummer, T. H. Jr., Deglycosylation of asparagine-linked glycans by peptide:N-glycosidase F. *Biochemistry* 1985, *24*, 4665–4671.

[7] Gorman, J. J., Wallis, T. P., Pitt, J. J., Protein disulfide bond determination by mass spectrometry. *Mass Spectrom. Rev.* 2002, *21*, 183–216.

[8] Roesli, C., Mumprecht, V., Neri, D., Detmar, M., Identification of the surface-accessible, lineage-specific vascular proteome by two-dimensional peptide mapping. *FASEB J.* 2008.

[9] Scheurer, S. B., Rybak, J. N., Roesli, C. *et al.*, Identification and relative quantification of membrane proteins by surface biotinylation and two-dimensional peptide mapping. *Proteomics* 2005, *5*, 2718–2728.

[10] Roesli, C., Neri, D., Rybak, J. N., *In vivo* protein biotinylation and sample preparation for the proteomic identification of organ- and disease-specific antigens accessible from the vasculature. *Nat. Protocols* 2006, *1*, 192–199.

[11] Rybak, J. N., Ettorre, A., Kaissling, B., Giavazzi, R. *et al.*, *In vivo* protein biotinylation for identification of organ-specific antigens accessible from the vasculature. *Nat. Methods* 2005, *2*, 291–298.

[12] Rybak, J. N., Roesli, C., Kaspar, M., Villa, A., Neri, D., The extra-domain A of fibronectin is a vascular marker of solid tumors and metastases. *Cancer Res.* 2007, *67*, 10948–10957.

[13] Castronovo, V., Waltregny, D., Kischel, P., Roesli, C. *et al.*, A chemical proteomics approach for the identification of accessible antigens expressed in human kidney cancer. *Mol. Cell. Proteomics* 2006, *5*, 2083–2091.

[14] Roesli, C., Elia, G., Neri, D., Two-dimensional mass spectrometric mapping. *Curr. Opin. Chem. Biol.* 2006, *10*, 35–41.

[15] Dziegielewska, K. M., Brown, W. M., Casey, S. J., Christie, D. L. *et al.*, The complete cDNA and amino acid sequence of bovine fetuin. Its homology with alpha 2HS glycoprotein and relation to other members of the cystatin superfamily. *J. Biol. Chem.* 1990, *265*, 4354–4357.

[16] Chin, C. C., Wold, F., The use of tributylphosphine and 4-(aminosulfonyl)-7-fluoro-2,1,3-benzoxadiazole in the study of protein sulfhydryls and disulfides. *Anal. Biochem.* 1993, *214*, 128–134.

[17] Pappin, D. J., Hojrup, P., Bleasby, A. J., Rapid identification of proteins by peptide-mass fingerprinting. *Curr. Biol.* 1993, *3*, 327–332.

